MOLECULAR DYNAMICS STUDY OF THERMAL CONDUCTIVITY OF BISMUTH TELLURIDE

By

SHIKAI WANG

A THESIS PRESENTED TO THE GRADUATE SCHOOL
OF THE UNIVERSITY OF FLORIDA IN PARTIAL FULFILLMENT
OF THE REQUIREMENTS FOR THE DEGREE OF
MASTER OF SCIENCE

UNIVERSITY OF FLORIDA

2013

To my Mom, for her kindness.
To my Dad, for his tolerance.
To my sister, for her loveliness.

ACKNOWLEDGMENTS

I would like to thank my parents and my little sister at this very beginning. I cannot enjoy my life without their both material and spiritual support all along. They show me one truth that no matter what trouble I have, families are always my solid supporter and biggest fans.

With no doubt, I must thank Dr. Youping Chen who provides me this opportunity to experience the happiness and sorrow of doing research and who will also fully support me to travel to IMECE conference in November.

I also thank Dr. Curtis Taylor for his interest in molecular dynamics simulation and willingness be my committee member and review my thesis work.

I thank my lab colleges: Liming Xiong, Ning Zhang, Shengfeng Yang, Xiang Chen, Rui Che, Chen Zhang, and Zexi Zheng for their technic supports and advices.

Special thanks is given to my ex-girlfriend for her sustained encouragement during the time we spent together. And I truly hope she will find her Mr. Right someday.

At last, I declare that I am an agnostic. But if there is God, for creating this wonderful world, I sincerely thank Him.

TABLE OF CONTENTS

page

LIST OF TABLES

LIST OF FIGURES

LIST OF ABBREVIATIONS

EMD	Equilibrium Molecular Dynamics
MD	Molecular Dynamics
NEMD	Non-equilibrium Molecular Dynamics
PBC	Periodic Boundary Condition
PMFP	Phonon Mean Free Path

Abstract of Thesis Presented to the Graduate School
of the University of Florida in Partial Fulfillment of the
Requirements for the Degree of Master of Science

MOLECULAR DYNAMICS STUDY OF THERMAL CONDUCTIVITY OF BISMUTH TELLURIDE

By

Shikai Wang

May 2013

Chair: Youping Chen
Major: Mechanical Engineering

Bismuth telluride (Bi_2Te_3) is one of the best thermoelectric materials at room temperature. Since the crystal structure of Bi_2Te_3 is very complicated and hard to be modeled, a new method based on a self-made orthorhombic lattice is applied to build atomic specimen in orthogonal boxes easily.

Generally in a molecular dynamics (MD) simulation, the thermal conductivity of Bi_2Te_3 is measured by using Green Kubo method which is an equilibrium method and able to calculate the whole thermal conductivity tensor in just one simulation. However, more detailed information could be obtained by applying direct method instead which is a non-equilibrium MD method, such as temperature distribution in a specimen or even near a grain boundary in a heat transfer which could give us further understandings of the thermal properties of Bi_2Te_3. Due to the large temperature gradient caused by the low thermal conductivity, the direct method based MD simulation of Bi_2Te_3 could be challenging. In this paper, with the interatomic potentials studied by Huang et al[2] and Qiu et al[8] appropriate heat fluxes are applied to the tests. And an analysis of finite-size effect shows the result which agrees with both experiment data and the result of Green Kubo method quite well.

Finally, the temperature distribution and Kapitza conductance of bi-crystal specimens with twin boundaries is studied which gives the conclusion that twin boundaries may not be able to generate very much heat resistance in Bi_2Te_3.

CHAPTER 1
INTRODUCTION

Bismuth Telluride

Nowadays, the unstoppable increase of energy consumption has been becoming a severe problem as fossil fuel, one of the main energy source, is less and less. For decades, people are seeking more alternative energy resources and thermoelectric material could be a good choice to collect energy which has been widely applied to solid-state cooling devices to convert electricity to heat and thermoelectric devices inversely to convert heat into electrical energy. Usually a good thermoelectric material should have not only high electrical conductivity but also low thermal conductivity.

Bismuth Telluride (Bi_2Te_3), considered as one of the best thermoelectric materials, has a very low thermal conductivity. And its alloys give high thermoelectric figure of merit, defined as $ZT = S^2\sigma T / K$, where S is the Seebeck coefficient, σ is the electrical conductivity, κ is the thermal conductivity, and T is the absolute temperature[12]. A material that can afford competitive performance must have a ZT value higher than 1 and a high merit ZT of 1.4 at 100℃ was reported in a p-type nanocrystalline BiSbTe bulk alloy[1]. Besides, at near room temperature (0℃ to 250℃), the best commercial thermoelectric materials for applications are still the Bi_2Te_3 based materials[12]. As stated in other publications[2,3], the thermal conductivity of Bi_2Te_3 is around 1~2W/mK based on the results of experiments and simulations.

The lattice of Bi_2Te_3 is mostly visualized as a layer structure[5] (Figure1-1) which has a rhombohedral crystal structure $(R\bar{3}m)$ and includes five atoms along the trigonal axis in the sequence of Bi-$Te^{(1)}$-$Te^{(2)}$-$Te^{(1)}$-Bi. The rhombohedral unit-cell parameters are $a_R = 10.473$ Å and $\theta_R = 24.159^\circ$[2]. Conventionally, Bi_2Te_3 also can be indexed in terms

of a hexagonal unit-cell with lattice parameters $a = 4.38$ Å and $c = 30.49$ Å[4] which contains three blocks and each block is a five-layer packet[2] with the atom sequence of $Te^{(1)}$-Bi-$Te^{(2)}$-Bi-$Te^{(1)}$.

Chemical bonds vary between layers. $Te^{(2)}$ and Bi atoms in adjacent layers are connected by covalent bonds. And $Te^{(1)}$ and Bi atoms in adjacent layers are linked by both covalent and ionic bonds. These two bonds are quite strong comparing to the bonding between $Te^{(1)}$ and $Te^{(1)}$ atoms in adjacent layers, which is just bonded by Van der Waals force[6].

For modeling convenience, a self-made unit (Figure 1-2) with orthogonal repeatable boundaries is applied. This base-centered orthorhombic crystal lattice also contains three blocks and each block has a five-layer-atom structure. Totally there are 30 atoms in this lattice structure and 2 atoms in each layer.

Molecular Dynamics

Regarding an atom as the basic rigid body, molecular dynamics (MD) is an approach that calculating the movements of a specific group of atoms to study material behavior by computer simulations. Generally, only molecular models and interatomic potentials are needed to achieve an MD simulation. After years of development, especially the enhancing performance of computers, MD simulation has been widely used in many areas, including material science. This paper mainly focus on the calculation of thermal conductivity by MD simulations. Generally, there are two major approaches to compute thermal conductivity: one is nonequilibrium MD (NEMD) method and the other one is equilibrium MD (EMD) method, such as the “direct method” and the Green-Kubo method respectively[7] which are the two most popular methods for computing thermal conductivity[7]. The direct method is applied by generate a

temperature gradient across the model which is very similar to an experimental case[7]. On the contrary, the Green-Kubo method calculates thermal conductivity through the heat fluctuation inside a simulation specimen which does not have a temperature gradient[7].

In this paper, all the conductivity computations are via the direct method since the Green-Kubo method has been tested on Bi_2Te_3 which gave rather good results[2,8] and the direct method application is still rare. The large temperature gradient as a necessity in the direct method may cause problems. However, as one benefit of this method by imposing temperature gradient, detailed information could be demonstrated directly, such as temperature distribution along the heat flux direction and near grain boundaries. Based on the potentials developed by Huang et al[2] and Qiu et al[8], the simulations will be applied to a group of models of different lengths and then calculate the thermal conductivity of infinite length (bulk thermal conductivity) by finite-size effect analysis.

Software

Lammps and VMD are two useful softwares when people deal with MD simulations.

Lammps is a powerful MD simulator which is distributed by Sandia National Laboratories as an open source code. Generally, Lammps is able to solve the problem when the potential, boundary conditions, and loads of an atomic model are set. Although large model which contains millions of atoms could be time consuming to reach convergence. As one essential advantage, Lammps is able to run either on single processors or in parallel which makes massive simulations be available.

VMD (Visual Molecular Dynamics) is a visualization program developed by the Theoretical and Computational Biophysics Group in University of Illinois at Urbana-Champaign. The purpose of using VMD is that this software is able to read Lammps' output files, i.e. xyz files, for displaying, animating, and analyzing. In this paper, most of the atomic schematics are output from VMD.

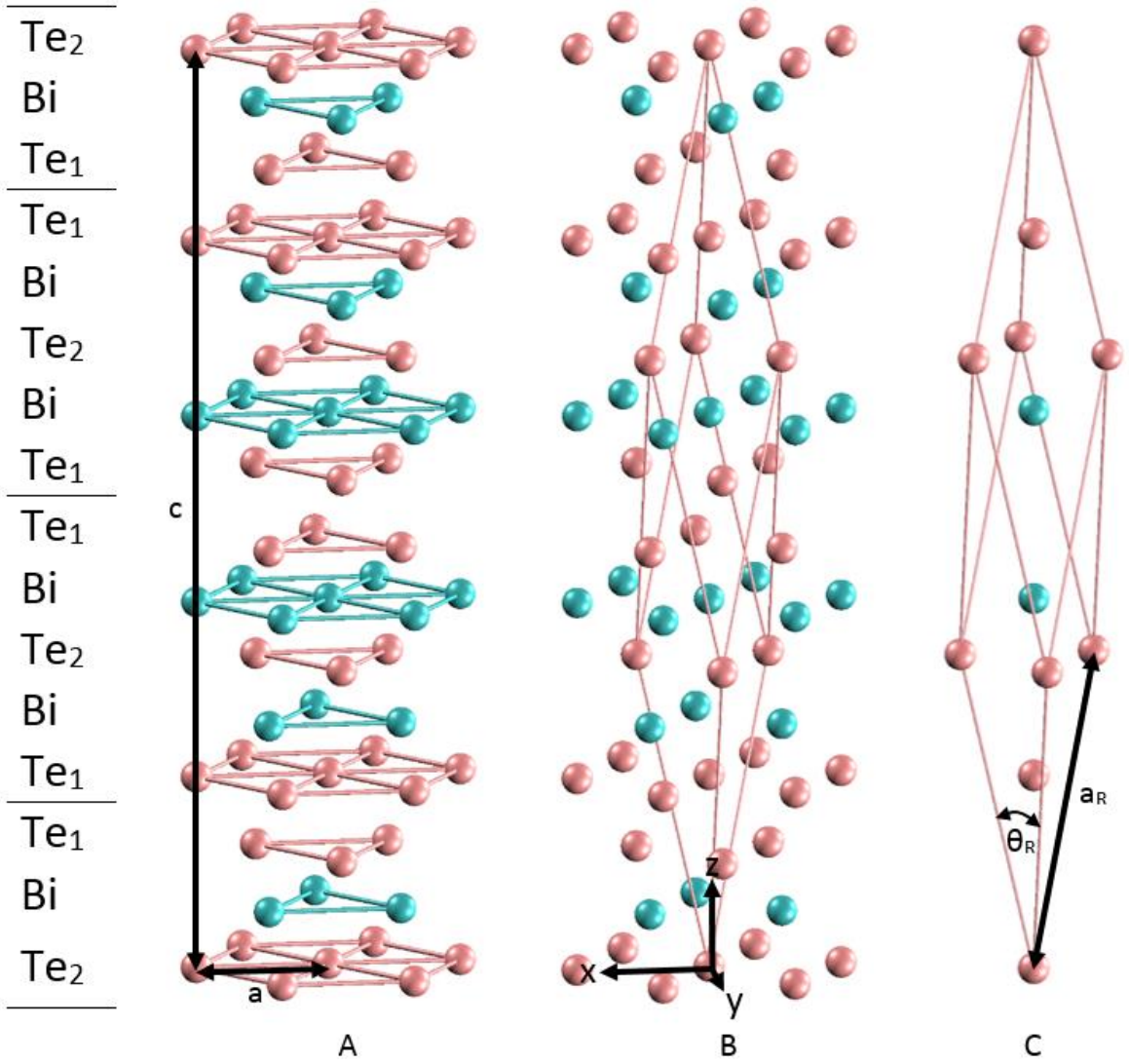

Figure 1-1. Figures show the relationship between a hexagonal lattice and a rhombohedral lattice of Bi_2Te_3. A) A conventional crystal structure in a hexagonal lattice which contains three blocks and each block has five layers. Lattice constants are marked in the figure. B) Hexagonal lattice is shown with a coordinate system and a corresponding rhombohedral lattice. C) The rhombohedral lattice of Bi_2Te_3 is shown with lattice constants.

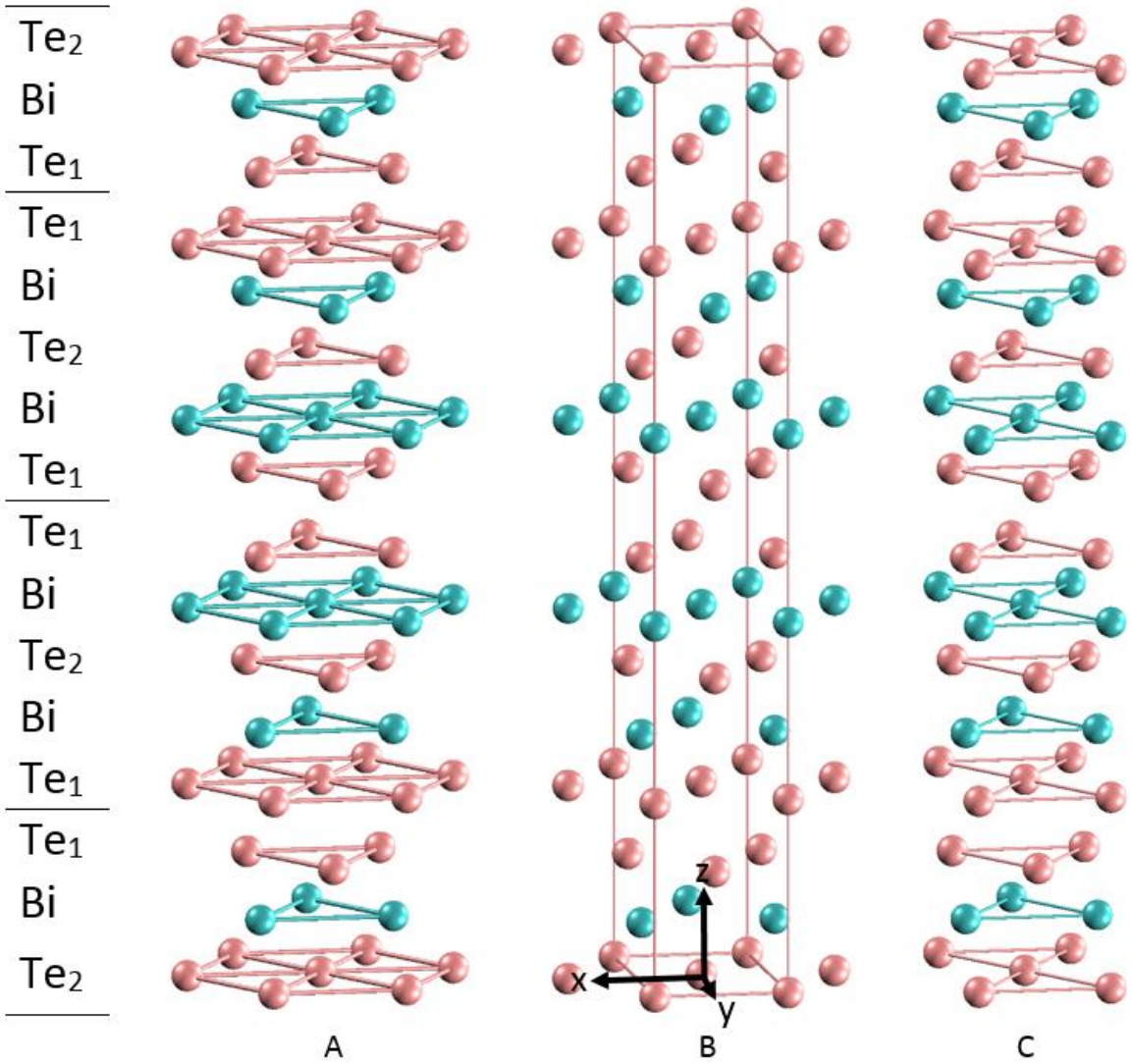

Figure 1-2. Figures illustrates the relationship between Bi_2Te_3's hexagonal lattice and self-made orthorhombic Lattice. A) A hexagonal lattice of bismuth telluride. B) A coordinate system and self-made lattice are shown in a hexagonal lattice. C) The structure of the self-made lattice which has a structure of base-centered orthorhombic crystal.

CHAPTER 2
MODELING WITH TWO POTENTIALS

Simulation Parameters

While modeling specimens, the first step is to determine the geometry parameters, such as length and cross-section. Different lengths and cross-sections may lead to different results which will be discussed.

The simulations in this paper are done with several specimens of different sizes. The thermal conductivity is calculated by the slope fitted from the temperature distribution data collected from slices along the length direction of the specimen. And each slice gives an average temperature of all the atoms within it. Although as stated in Ref. 7, the cross section did not show strong effect on simulation result. But in my simulations, if a too small cross section is applied, temperature gradient could be obviously affected. Specimen with small cross-section could not provide enough atoms in each sampling slices for data collection. On the contrary, big one could consume much more computation resources. As tested for many times, the cross-section of $5.98 nm^2$ should be a good choice.

Except cross section, model length will influent the result as well. Short specimen gives less sampling slices which may not have an accurate result but makes large temperature gradient available. On the other hand, long specimen gives enough sampling slices but temperature gradient would remain very small, since small temperature gradient represents small heat flux which could be easily affected by system error. Besides, in order to employ finite size effect, the total length should not be too much bigger than the phonon mean-free path of Bi_2Te_3 which is only around 2 nm[9]

at 300K. Under these considerations, a range of 18nm to 60nm was appropriately selected.

Prior work[7] has indicated that loading different heat flux could also affect the MD simulation result. Low heat flux could be affected by comparable system noise and lose lots of accuracy. However, high heat flux model could also be inaccurate that generate too high source temperature which beyond potential's limit and may let sink atoms go negative energy value which results in simulation fail. Shown in Figure 2-1, larger heat flux results in smoother curve. But in the last diagram, the temperature in heat source is beyond the potential limit 500K. The reason that heat current instead of heat flux is used in the diagrams is that all the models have the same cross section and thus heat current comparison is identical to heat flux comparison.

Bi_2Te_3-based materials dominate at relatively near room temperature (0℃ to 250℃)[1], and in addition, the Debye temperature of Bi_2Te_3 is 162K[10]. The simulation temperature should be higher than the Debye temperature and thus a temperature of 400K (127℃) was chosen during all the simulations.

Orthogonal Simulation Box Model

In the prior works about Bi_2Te_3 MD simulation, orthogonal specimens were hardly been reported mainly because of the difficulties in Bi_2Te_3 modeling which brought by its complicated crystal structure. In many cases, an orthogonal simulation box could be much simpler to model and control. Based on the self-made base-centered orthorhombic crystal structure (Figure 1-2), specimens of different lengths along z-direction from 18nm to 60nm and the same cross-section of 5.98 nm^2 were built with repeatable orthogonal boundaries. (Figure 2-2)

Besides, bi-crystal models with twin boundaries were built with the orthogonal unit cell as well. The only difference between the bi-crystal and single-crystal models was to modifying the y values of a half of all atoms' positions. The cross-section remains the same and lengths along z-direction were selected to be 24nm and 36nm. In Figure 2-3, the overlapping of scanned image and atomic model is quite precise and hence the bi-crystal model is ready to use.

Potentials

Since Bi_2Te_3 is a relatively new material for MD study, there are only two available potentials so far which are from the previous works of Huang et al[2] and Qiu et al[8]. Particularly, the latter is based on Morse potential and Coulomb force together and the former potential combines Morse potential, cosine square angular potential, and Coulomb force. The angular potential also makes the potential developed by Huang et al [2] more difficult to be employed to atomic models, especially in simulation boxes of periodic boundary condition. It is important that the cutoff of each pair was chosen to be a little larger than the specific atoms' distance between and the cutoff radius of the electrostatic terms is adjusted from 12Å to 10Å as recommended by Huang in our private contact. Table 2-1 gives the detail information of the cutoffs of each pair listed in his potential.

Since all the simulations in this paper are thermal tests, thus the atoms' positions almost remain stable. To deal with the adjacent/same layers pair, the atoms in each block in a sequence of $Te^{(1)}$-Bi-$Te^{(2)}$-Bi-$Te^{(1)}$ were renamed as $Te^{(1)(1)}$-$Bi^{(1)}$-$Te^{(2)}$-$Bi^{(2)}$-$Te^{(1)(2)}$, and hence there were five types of atoms. Therefore, to distinguish adjacent/same layers pair became very easy.

When applying angular potentials, some more effort are needed. In Lammps, to make the angles readable to the program, all the angles must be listed by the three indexes of the atoms in that specific angle. In order to list these indexed out, the method that I applied is to find the center atom one by one, then search the nearest atoms that belong to the angles for each center atom, and finally all the angles could be located in such approach. The larger the model is, the significant longer searching time will be needed. (Figure 2-4)

In most cases, periodic boundary condition (PBC) should be employed in an MD thermal simulation. To apply angular potential in a PBC case, First, I wrap the whole specimen with atoms which are located in the neighbor boxes. Then mark these atoms with the index information of their mapping atoms in the current simulation box. At last, use the method stated in last paragraph and hence all the angles would be listed in a data file which could be ready to associate with the original model which does not have wrapping atoms.

The total angle amount in a PBC model could be expressed as $N_{angle} = 8.4N_{atom}$, where N_{angle} is the amount of angles and N_{atom} is the amount of total atoms.

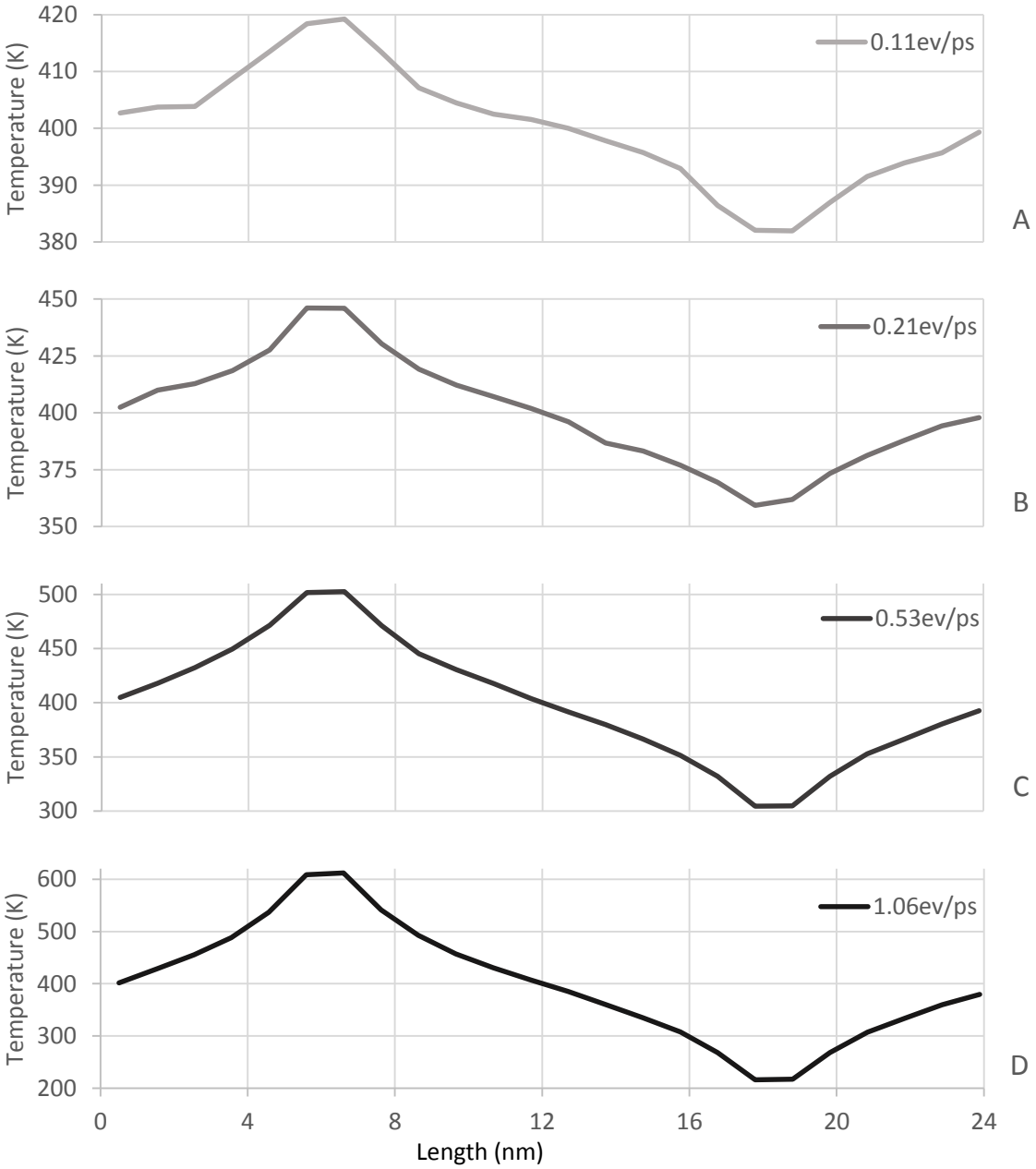

Figure 2-1. Diagrams above give the temperature distributions under different heat currents applied. All of these models share the same length and cross section. In each diagram, the highest partial indicates the location of heat source and the lowest one indicates the location of heat sink.

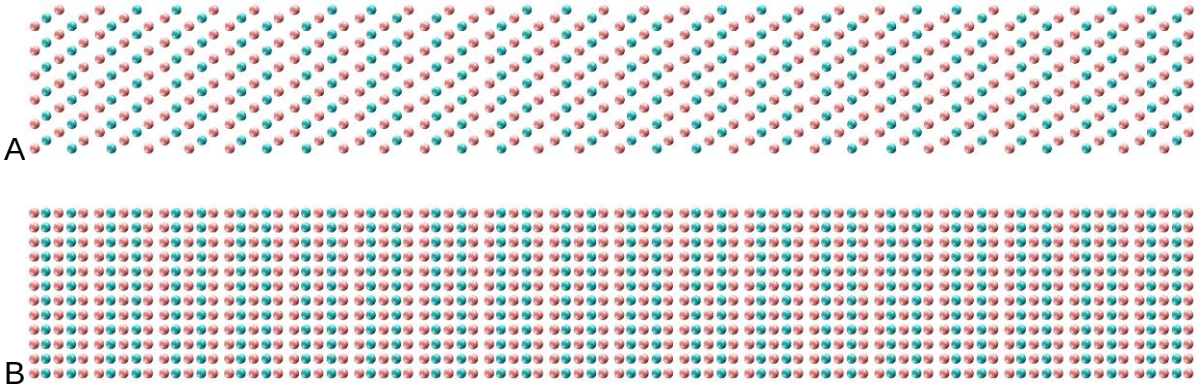

Figure 2-2. Figures show an 18nm atomic model applied in the simulation. A) X-direction view of an 18nm single-crystal model. B) Y-direction view of the same model.

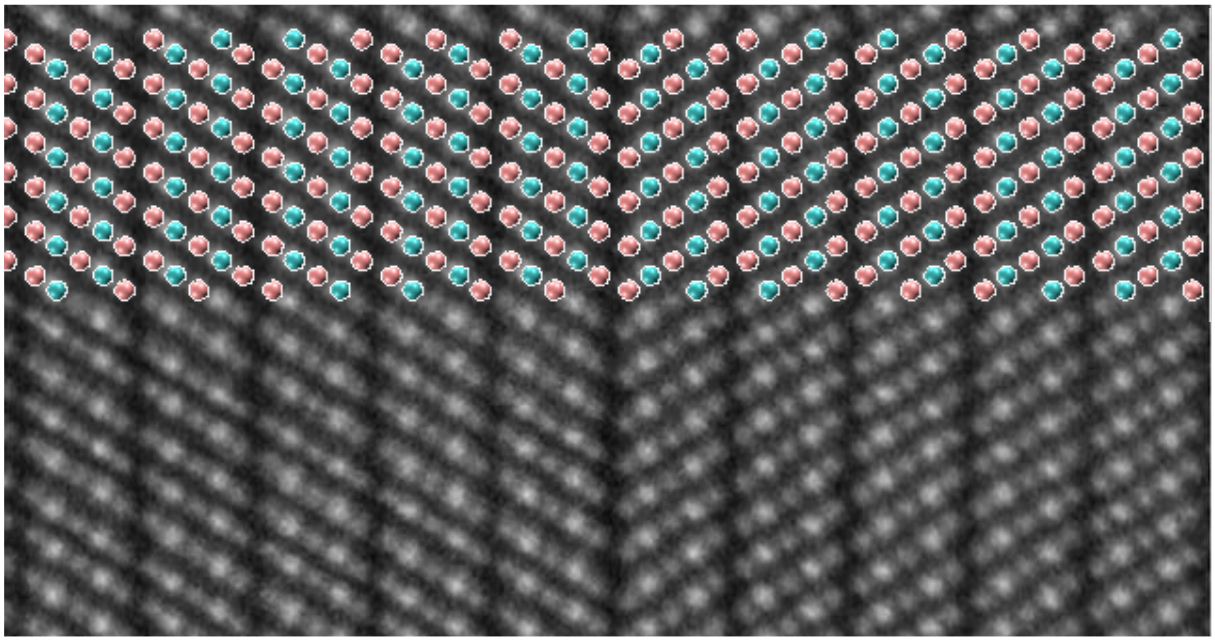

Figure 2-3. The color atoms are a part of the bi-crystal model. The blur background picture is HAADF-STEM image of the (0001) basal twin projected along $[2\bar{1}\bar{1}0]$ direction[4].

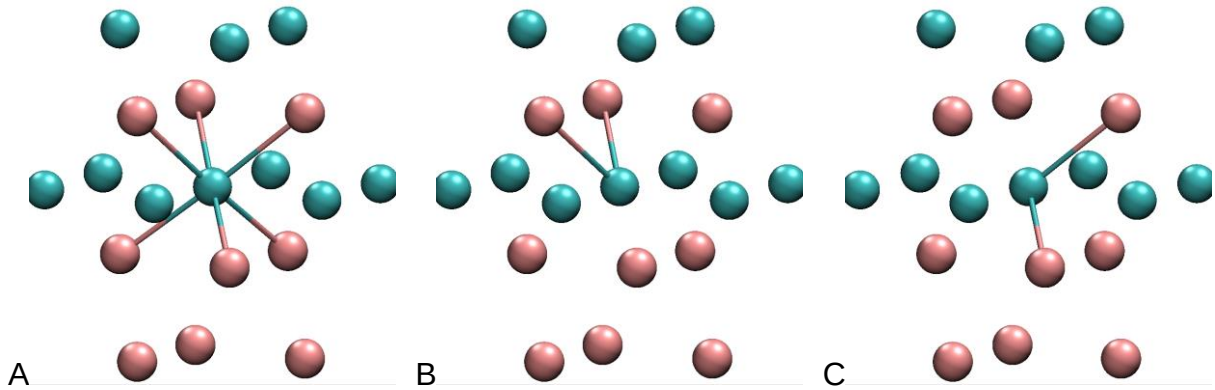

Figure 2-4. Figures show the brief procedure to search angles. A) The green atom is the center atom, the bonded red atoms are to be found. B) One possible angle type (adjacent layer angles). C) The other possible angle type (three adjacent layer angles).

Table 2-1. Table of additional cutoffs for Huang's potential[2]

Interaction	Cutoff (Å)
$Te^{(1)}$-Bi (adjacent layers)	4.5
$Te^{(2)}$-Bi (adjacent layers)	4.5
$Te^{(1)}$-$Te^{(1)}$ (adjacent layers)	4.5
Bi-Bi (same layer)	5.5
Coulomb force (All atoms)	10

CHAPTER 3
MD SIMULATION OF SINGLE-CRYSTAL MODEL

Relaxation

The first step of an MD simulation after modeling is to relax the system which is a processing that minimizes the total energy of the whole system and let the system get to an equilibrium condition. The method of applying relaxation process is quite simple which is to run the simulation without any load for a period, such as 1ns, with NVE ensemble. Generally, the model could not perfectly consist with the potential. As shown in Figure 3-1, the system temperature fluctuate very severely at beginning and become stable after a while which gives a typical relaxation process. Usually the time for relaxation varies in different situations.

In this paper, the relaxation time for all simulation cases is 0.25ns and the time step is set to 0.25fs, hence totally one million time steps will be undertaken during the relaxation. Then the temperature of the specimen will be increasing to 400K gradually with NVT ensemble. After the system temperature reach 400K, keep the simulation running with NVE ensemble for another 0.25ns to eliminate probable unstable factors as many as possible.

Direct Method

Background

As introduced in chapter 1, direct method is an NEMD method to calculate thermal conductivity and it is very similar to an experimental measurement. While employing direct method, either temperature or heat flux could be loaded on the system to generate an appropriate temperature gradient. When the two systems both reach stable status, the same result should the simulations give based on these two loading

approaches (Figure 3-2). In my thesis work, all simulations are employing the energy loading approach, as it is easier to compute the heat flux in the specimen and the reference temperature could be easily determined as 400K which is initially fixed. As shown in Figure 3-3, same amount of energy is added to the heat source and subtracted from the heat sink every time step, and hence the whole system remains energy conserved. J is the heat flux which is measured in [W/m^2] and defined as:

$$J = \frac{160.22\Delta\varepsilon}{2A\Delta t} = \frac{160.22e}{2A} \tag{3-1}$$

Where $\Delta\varepsilon$ is the energy added to/subtracted from the system's heat source/sink which is measured in [ev], A is the cross section of the specimen, Δt is the time step used in the simulation, and hence e is the added/subtracted energy every time step as a convenience to edit Lammps' input file. The coefficient in this equation means the unit conversion from [ev] to [J]. The arrows in Figure 3-3 show the direction of the heat flux and the thermal conductivity could be calculated from the Fourier's law:

$$J = -\kappa\nabla T \tag{3-2}$$

Where κ is thermal conductivity and ∇T is temperature gradient. The negative sign in this formula means the directions of heat flux and temperature gradient are opposite. Thus, the thermal conductivity could be expressed in this way:

$$\kappa = \frac{160.22e}{2A\left|\nabla T\right|} \tag{3-3}$$

Where the absolute value of temperature gradient is used to ensure the thermal conductivity remain a positive value.

It is notable that while a large temperature gradient applied to the system, strong nonlinear behavior will appear and which could make this method invalid. Even with

relative small temperature gradient, there still will be nonlinear behaviors at boundaries of source and sink caused by boundary scattering[7]. In some materials, i.e. silicon, this boundary nonlinearity is very significant.

Simulation of Nano Scale Specimen

As mentioned in the first chapter, at near room temperature (0℃ to 250℃), it is hard to find a competitor to Bi_2Te_3 based material for its outstanding thermoelectric property. Thus, the reference temperature of 400K was selected which is also higher than the Debye temperature 162K[10].

During the simulation, the kinetic energy of all atoms are collected slice by slice, and the thickness of each slice is 5nm which contains 90 atoms in total. The temperature of each slice could be computed with the relationship between kinetic energy and temperature:

$$E = \frac{3}{2} k_B T \tag{3-4}$$

Where E is the kinetic energy of all the atoms in each slice, k_B is the Boltzmann's constant, and T is the needed temperature.

In thermal simulation with direct method, long time average is usually needed to reduce statistically fluctuation[11] after stable status achieved. First the relaxed system runs for 2 million time steps (0.5ns) to reach a stable condition, then two data collections are applied during the following 4 million time steps, each data collection runs for 2 million time steps respectively. In Figure 3-4, the orange dots and the blue dots show the temperature averaged from the two collections. The well overlapped pattern indicate that the system has been reach a stable status after the 0.5ns running before the collection process starts.

The temperature gradient needs to be calculated before the thermal conductivity computation. Very obvious nonlinear curves present near the heat source and heat sink boundaries which are the result of strong phonon boundary scattering near that regions (Figure 3-2 and 3-4), but the Fourier's law could still be employed to the linear regions respectively at intermediate part of the specimen and the part near the periodic boundary along the length direction. The temperature gradient is given by the two fitted slopes from these two regions. Apply with the formulas which introduced in the last section, the thermal conductivities of all the single-crystal models are calculated and listed in Table 3-1.

In the next section, finite size effect will be introduced in detail, and which could give an approach to approximate the thermal conductivity of infinite specimen which could be regarded as the Bi_2Te_3's bulk thermal conductivity.

Finite Size Effect

The thermal conductivity could be affected by the size of the simulation box along the heat flux direction when the specimen length is not significantly longer than the material's phonon mean free path, this phenomenon is named finite size effect, also known as the Casimir limit[12]. Generally, smaller specimen dimension gives lower thermal conductivity. In ideal single-crystal, the limited effective thermal conductivity could be expressed in such way[13]:

$$\frac{1}{\kappa_{eff}} = r + \frac{R_{ss}}{L_z} \tag{3-5}$$

Where κ_{eff} is effective thermal conductivity and its inverse is the effective thermal resistance per unit length, r is the material bulk thermal resistance per unit length which

is a material dependent property and $r = 1/\kappa_{bulk}$, R_{ss} is the boundary thermal resistance, including both heat source and sink boundary resistance, and L_z is the simulation box length. Thus, this expression indicates that the total effective thermal resistance equals to the sum of material thermal resistance and boundary thermal resistance and that obviously the inverse of the effective thermal conductivity has a linear relationship to the inverse of the specimen's size. When the length of the specimen L_z gets infinity, κ_{eff} could clearly be identical with κ_{bulk} .

In further detail, kinetic theory[7] give an equation to determine thermal conductivity:

$$\kappa = \frac{1}{3} cvl \tag{3-6}$$

Where c is the material specific heat, v is the sound velocity in the material, and l is the phonon mean free path. Insert this expression into Equation 3-5 gives:

$$\frac{1}{l_{eff}} = \frac{1}{l_{\infty}} + \frac{R_{ss} cv}{3L_z} \tag{3-7}$$

Where l_{eff} is the effective phonon mean free path, l_{∞} is the bulk phonon mean free path. In Ref. 7, it has been indicated that $R_B cv = 12$. And the specific heat could be expressed as:

$$c = \frac{3}{2} k_B n \tag{3-8}$$

Where k_B is the Boltzmann's constant, n is the number density of atoms in the system and in Bi_2Te_3, $n = 29.57\,\text{nm}^{-3}$. Thus, substituting Equation 3-6 and Equation 3-8 into Equation 3-5 gives:

$$\frac{1}{\kappa_{eff}} = \frac{2}{k_B n v l_\infty} + \frac{R_{ss}}{L_z} \tag{3-9}$$

Result

Thermal conductivity computed from different length specimens are listed in Table 3-1. Obviously, longer specimen gives larger thermal conductivity as finite size effect said. And also, from the results from two potentials, Huang's potential[2] gives larger results.

Based on the finite size effect, the bulk thermal conductivity could be extrapolated from the finite size results of different lengths. In Figure 3-5, when the inverse of L_z is zero, that is, L_z gets to infinity, the inverse of the value on the vertical axis (the intercept) would be the bulk thermal conductivity which is 1.566W/mK for Huang's potential[2] and 0.609W/mk for Qiu's potential[8]. Besides, the result of Green Kubo method is around 1W/mK and result of experiment is about 2W/mK[2,3]. Compared with these results, this value is quite close to those. In other words, the accuracies of the two potentials are acceptable.

In the next Chapter, a set of bi-crystal specimen is employed with the same simulation procedure and the influence of twin boundary to the temperature distribution is discussed.

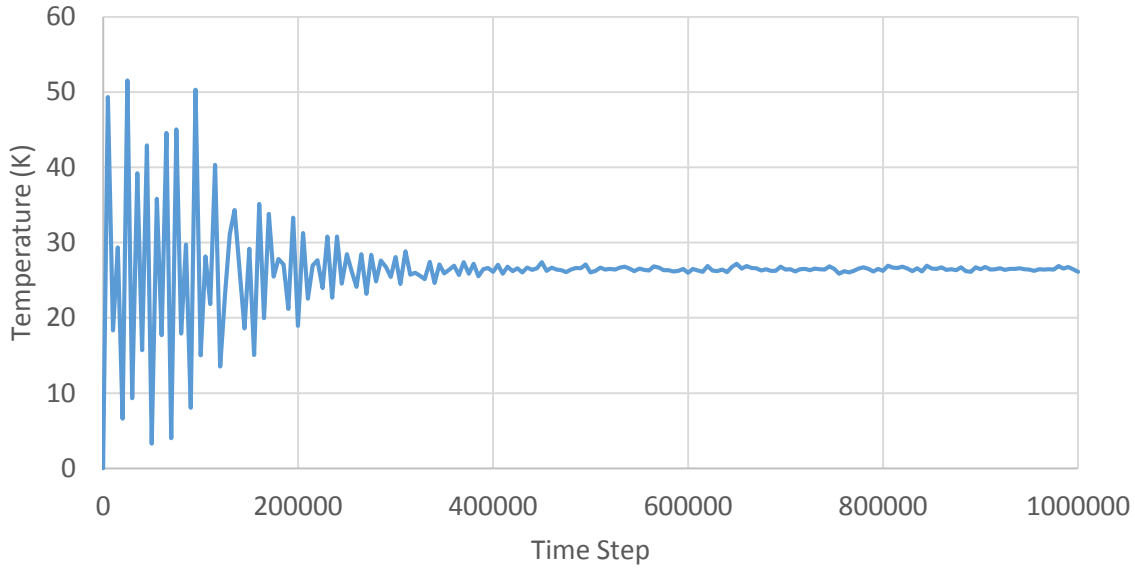

Figure 3-1. Diagram shows the stabilizing temperature. After 1000,000 steps, the system temperature has been nearly constant around 27K.

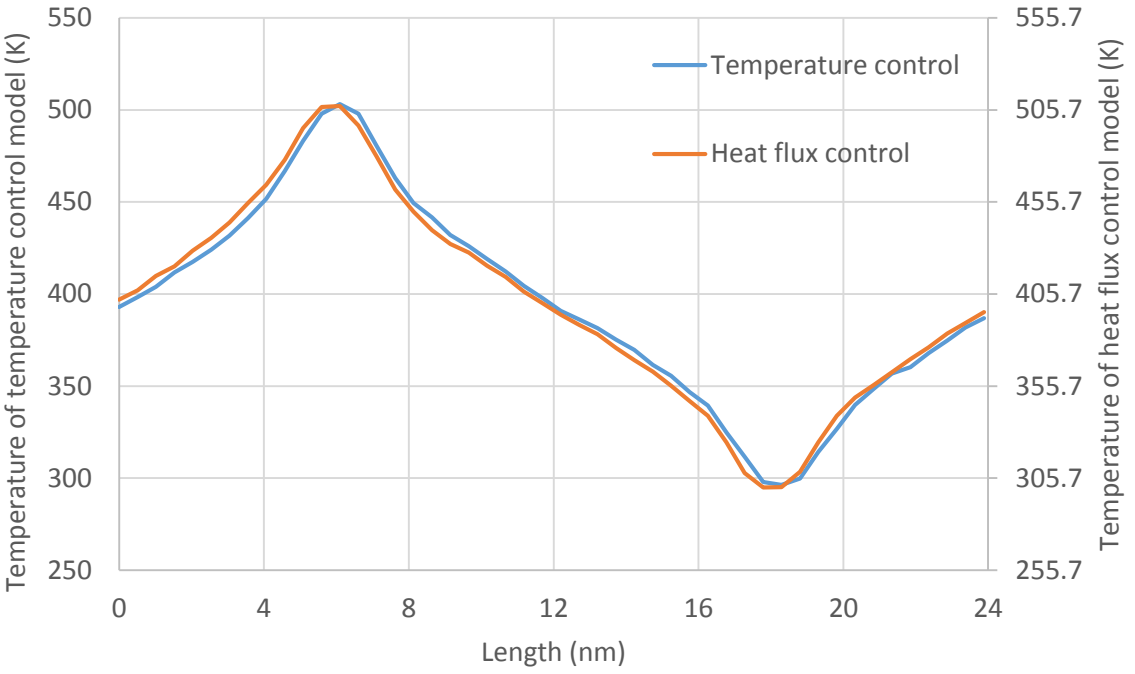

Figure 3-2. This diagram gives that results of adding temperature and adding heat flux are very close. And the difference of these two models' average temperature is 5.7K which could be modified by adjusting the load of temperature control method.

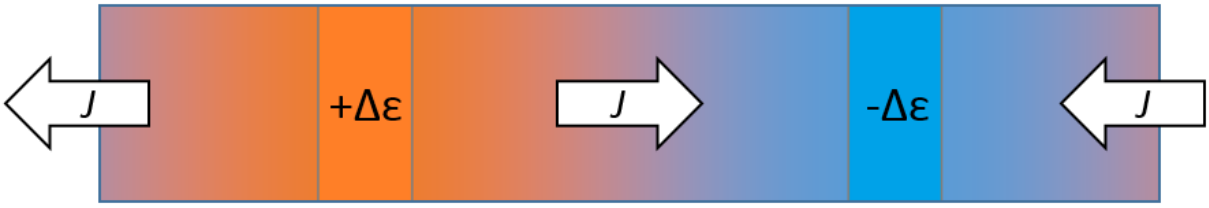

Figure 3-3. A sketch of direct method under periodic boundary condition. Where J is heat flux, energy of $\Delta\varepsilon$ is added and subtracted from the heat source and sink respectively. Thus a temperature gradient could be established.

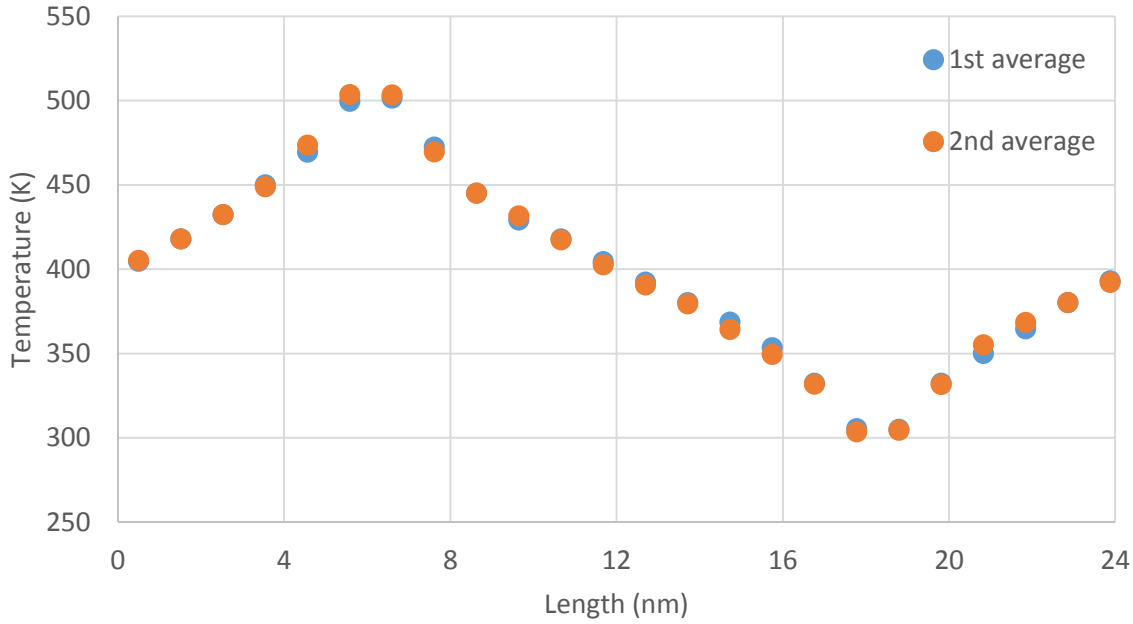

Figure 3-4. This diagram shows the comparison of two averages in a 24nm model. Each average is computed through 2 million time steps.

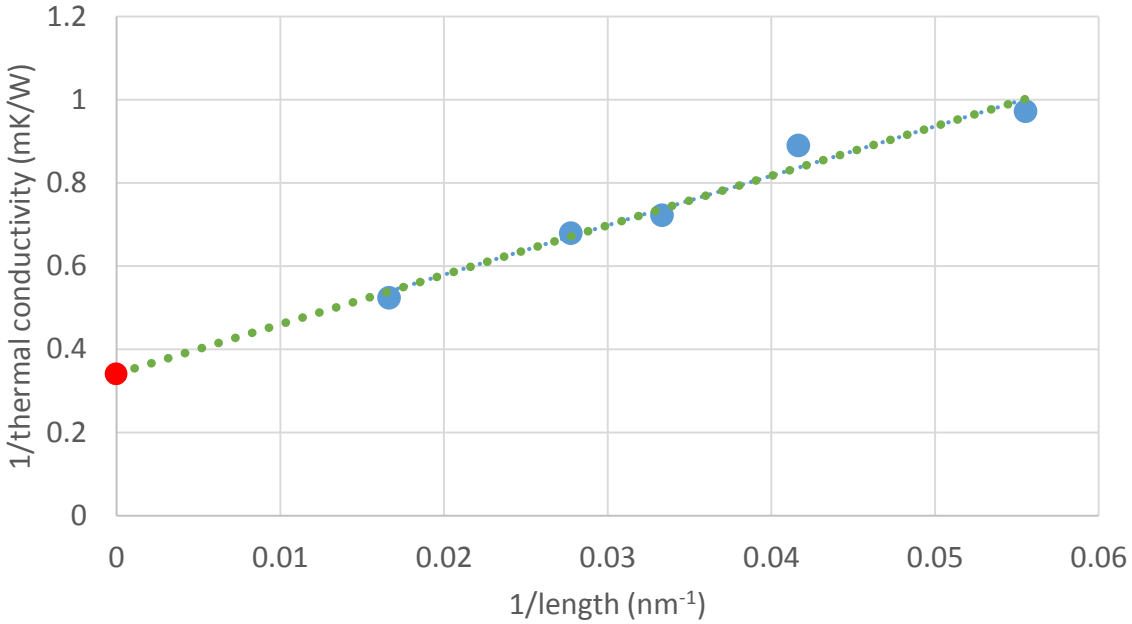

Figure 3-5. Diagram gives the extrapolation of bulk thermal conductivity. The blue dots are the MD result of finite size thermal conductivity and the red dot is the extrapolated point. Note that the horizontal and vertical axes are labeled in the inverse of length and thermal conductivity. These data are based on the potential developed by Huang et al[2].

Table 3-1. Table of thermal conductivities of single-crystal bismuth.

Length (nm)	Thermal conductivity (W/mK)
Huang's potential[2]	
18	0.550
24	0.672
30	0.800
36	0.789
60	1.003
+ ∞	1.566
Qiu's potential[8]	
18	0.206
24	0.244
30	0.273
36	0.314
+ ∞	0.609

CHAPTER 4
MD SIMULATION OF BI-CRYSTAL MODEL

Simulation Procedure

The relaxation process applied on bi-crystal model is the same as the one did on single-crystal model.

In Figure 4-1, atoms near twin boundary become messy after relaxation in the model associated with Qiu's potential[8]. However, this twin boundary structure based on Huang's potential[2] keeps a stable status during the simulation. Hence, the bi-crystal thermal simulation will be employed in the models based on Huang's potential[2] only.

Still, the direct method is employed here (Figure 4-2). The goal of this simulation is to observe some possible effects on temperature distribution generated by the twin boundary. Theoretically, phonon will be scattered when going through a grain boundary. Locally at this interface, there will be an additional thermal resistance and hence thermal conductance as its inverse, named Kapitza conductance which have this following expression[14]:

$$J = \sigma_K \Delta T \tag{4-1}$$

Where J is the heat flux, ΔT (not ∇T) is the temperature discontinuity at the interface, and σ_K is the Kapitza conductance whose inverse $R_K = 1/\sigma_K$ is Kapitza resistance.

Result

The measurement applied on bi-crystal model is the same as the one did on single-crystal model except for the finite size effect analysis. With 120 and 180 slices along the length direction, the results of collected temperature are shown in Figure 4-3 and 4-4.

Very slight difference is found between the curves of single- and bi-crystal models. However, the discontinuous slope of temperature could be observed. The intercepts at twin boundary of fitted lines are calculated which are derived from the temperature data on both left and right side of grain boundary. The difference of the two intercepts is regarded as the temperature discontinuity at the interface. The heat flux inside the specimen is 14.3GW/m^2 in both two twin boundary models. Therefore, the Kapitza conductance could be computed from Equation 4-1 which gives 1.94GW/m^{2}K and 1.19GW/m^{2}K respectively in 24nm and 36nm models.

Recall the Equation 3-5, similar equation could be achieved for twin boundary crystal:

$$\frac{1}{\kappa_{tw}} = \frac{1}{\kappa_{bulk}} + \frac{R_{ss}}{L_z} + \frac{2}{\sigma_K L_z} \tag{4-2}$$

Where κ_{tw} is the resultant thermal conductivity of specimen with twin boundaries, the summation of first and second terms on the right hand side is identical to the inverse of κ_{eff} in the Equation 3-5, and the numerator 2 in the third term accounts for the fact that there are two grain boundaries in the specimen of length L_z. Therefore, the idea of this equation is that the overall thermal resistance is equal to the summation of material thermal resistance, finite size boundary resistance and grain boundary thermal resistance.

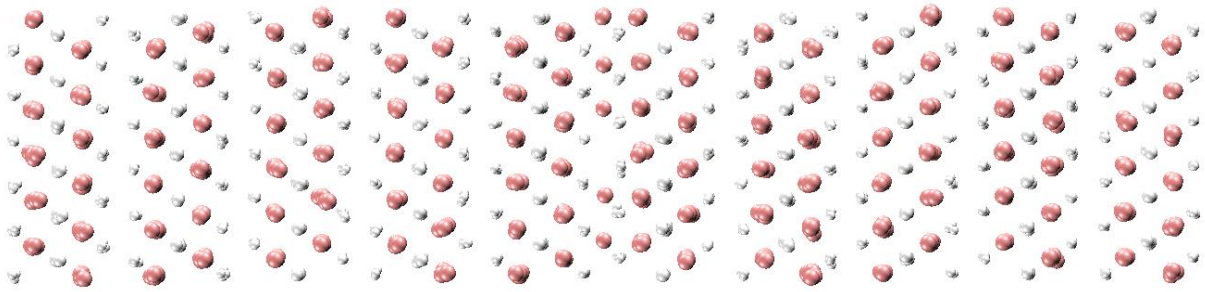

Figure 4-1. Figure above presents the atom arrangement of a PBC bi-crystal model associated with Qiu's potential[8] after relaxation. The twin boundary (in the middle of the figure) structure is not stable.

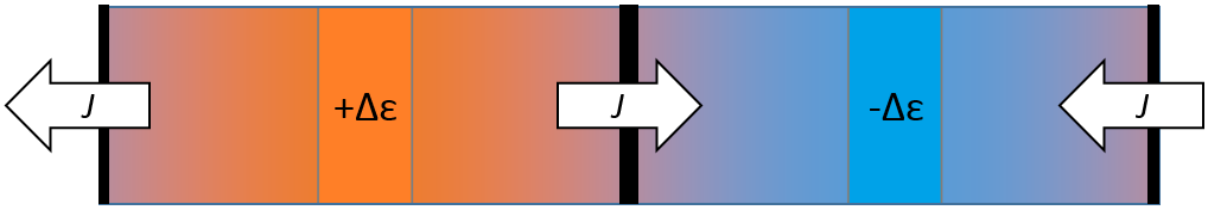

Figure 4-2. Similar to Figure 3-3, this figure illustrates the direct method model with grain boundary, where the black belts are the location of twin boundaries.

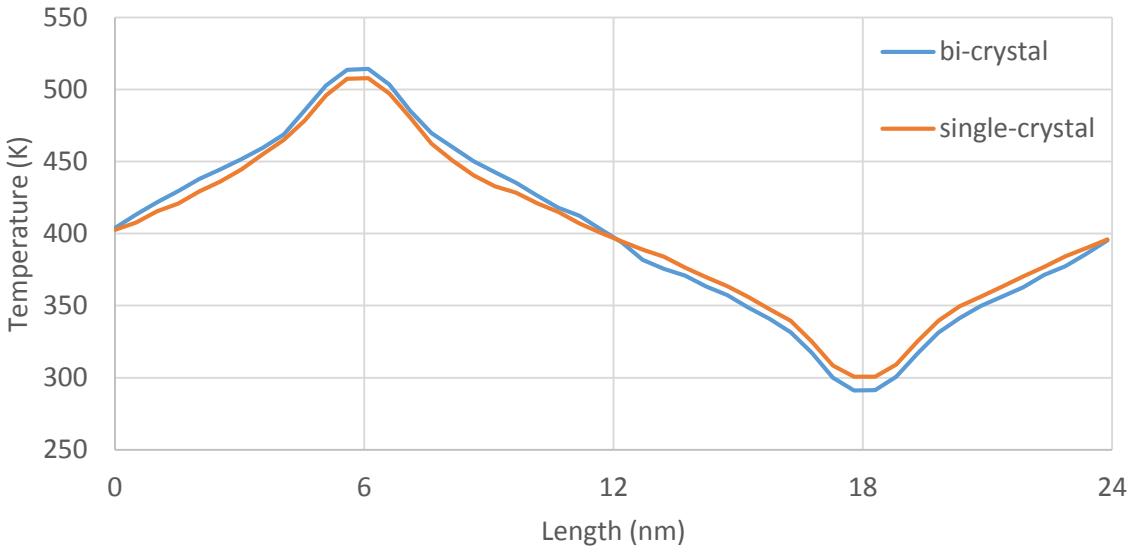

Figure 4-3. From the comparison of temperature distributions of two 24nm models, the temperature gradients are different near the twin boundary. The boundary also contributes to higher heat source temperature and lower heat sink temperature. Thus generally, the twin boundary do affects the thermal transport.

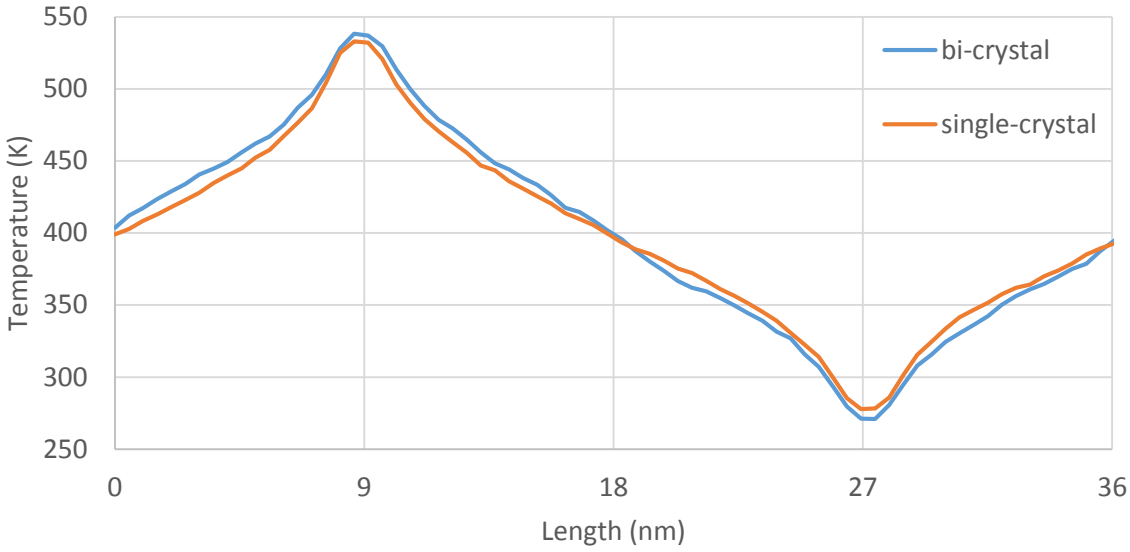

Figure 4-4. Similar to the 24nm model comparison in Figure 4-3, slightly differences are generated by the twin boundary.

CHAPTER 5
CONCLUSION AND DISCUSSION

So far, potential from Ref. 2 and Ref. 8 have been tested in direct method simulations. Compare with the Bi_2Te_3 thermal conductivity from other people's publications, it is no doubt that both of the potentials give reasonable results.

In Ref. 2, it is said the cutoff of Coulomb force is 12 angstrom. But actually this cutoff could result in a disorder model that all the blocks are dislocated along each other. By private contact, the cutoff was suggested as 10 angstrom and which stabilize the model. The complexity of this potential[2] may bring issue that the running time is longer than the potential in Ref. 8. The compute speed could be increased a little by pre-building the neighbor list, which was suggested by Huang as well. With these modification, this potential could be promising.

In this paper, a low cross-plane thermal conductivity of bismuth telluride has been achieved. But some error could still exist which may due to the small amount of sampling slices or relatively low heat flux. Also the error may come from the potential itself. Generally, comparing with the results of experiment and Green Kubo simulation, the result in this paper is acceptable.

In Ref. 16, a relatively high thermal conductivity of single crystal model associated with potential in Ref. 8 was given. It is interesting to notice a very large cutoff of pair interactions is chosen as 30Å, and they said this value is from the Ref. 8 of this paper. However, I cannot find the words about this large cutoff in Ref. 8. Their result seems questionable.

This MD simulation gives the result that twin boundary may not be able to strongly influence the heat conduction of bismuth telluride. It is interesting to see that

the Kapitza conductance value is very close to the one of some silicon grain boundary stated in Ref. 14 where very significant temperature drops appear at the grain boundaries. In addition, from Equation 4-2 we have

$$\frac{\kappa_s}{\kappa_{tw}} = 1 + \frac{2\kappa_s}{\sigma_K L_z} \tag{5-1}$$

Where κ_s is the single crystal thermal conductivity which is numerically equals to the κ_{eff} in Equation 4-5. From this equation, it is understandable that thermal conductivity will undoubtedly decrease when grain boundary exist since the ratio on the left hand side will always larger than one. And how much thermal effect could grain boundaries have depends on the ration of material thermal conductivity and boundary thermal resistance which is exactly the second term on the right hand side. In silicon, the grain boundaries mentioned in Ref. 14 could have a very large ratio. In bismuth telluride, however, this ratio remains much smaller than one and hence there is $\kappa_s \approx \kappa_{tw}$. An alternate expression of this equation has been stated in Ref. 15.

When applying direct method, heat flux could be approximately calculated before simulation by Fourier's law from the expected temperature gradient and experimental thermal conductivity. However, if the potential is not good enough, this method could bring trouble such as an unexpected temperature gradient. Also, the strong nonlinearity regions at heat source and sink could bring difficulties to finding proper temperature gradient. But pre-determined heat flux could always be a choice.

LIST OF REFERENCES

1. B. Poudel, Q. Hao, Y. Ma, Y. C. Lan, A. Minnich, B. Yu, X. Yan, D. Z. Wang, A. Muto, D. Vashaee, X. Y. Chen, J. M. Liu, M. S. Dresselhaus, G. Chen, and Z. F. Ren, Science 320, 634 (2008)

2. B. L. Huang and M. Kaviany, Phys. Rev. B 77, 125209 (2008)

3. P.A. Sharma, A.L.L. Sharma, D.L. Medlin, A.M. Morales, N. Yang, M. Barney, J. He, F. Drymiotis, J. Turner, and T.M. Tritt, Phys. Rev. B 83, 235209 (2011).

4. D. L. Medlin, Q. M. Ramasse, C. D. Spataru, and N. Y. C. Yang, J Appl. Phys. 108, 043517 (2010).

5. J. Drabble and C. Goodman, J. Phys. Chem. Solids 5, 142 (1958).

6. Y. Tong, F. J. Yi, L. S. Lui, P. C. Zhai, and Q. J. Zhang, Comput. Mater. Sci. 48, 343 (2010).

7. P.K. Schelling, S.R. Phillpot, P. Keblinski, Phys. Rev. B 65, 144306 (2002).

8. B. Qiu and X. Ruan, Phys. Rev. B 80, 165203 (2009).

9. N. Peranio, O. Eibl, and J. Nurnus, J. Appl. Phys. 100, 114306 (2006).

10. G. E. Shoemake, J. A. Rayne, and R. W. Ure, Phys. Rev. 185, 1046 (1969).

11. G. Chen, Nanoscale Energy Transport and Conversion: A Parallel Treatment of Electrons, Molecules, Phonons, and Photons (Oxford University Press, New York, New York, 2005).

12. H. B. G. Casimir, Physica 5, 495 (1938).

13. J. Michalski, Phys. Rev. B 45, 7054 (1992).

14. P. K. Schelling, S. R. Phillpot, and P. Keblinski, J. Appl. Phys. 95, 6082 (2004).

15. S. Aubry, C. J. Kimmer, A. Skye, and P. K. Schelling, Phys. Rev. B 78, 064112 (2008).

16. K. Termentzidis, O. Pokropyvnyy, M. Woda, S. Xiong, Y. Chumakov, P. Cortona, and S. Volz, J. Appl. Phys. 113, 013506 (2013).

BIOGRAPHICAL SKETCH

Shikai Wang was born in Weinan, Shaanxi, China in 1989.

From 2007 to 2011, he studied in Huazhong University of Science and Technology, Wuhan, China. And in 2001, He graduated with a degree of Bachelor of Science in Energy and Power Engineering.

From 2011 to 2013, Shikai was enrolled in University of Florida, FL, US to pursue a master's degree in the Department of Mechanical and Aerospace Engineering. Since 2012, Shikai has worked in Dr. Youping Chen's lab doing research on molecular dynamics simulation.